# REPORT 1061

## EFFECT OF INITIAL MIXTURE TEMPERATURE ON FLAME SPEED OF METHANE-AIR, PROPANE-AIR, AND ETHYLENE-AIR MIXTURES [1]

By Gordon L. Dugger


### SUMMARY

*Flame speeds based on the outer edge of the shadow cast by the laminar Bunsen cone were determined as functions of composition for methane-air mixtures at initial mixture temperatures ranging from —132° to 342° C and for propane-air and ethylene-air mixtures at initial mixture temperatures ranging from —73° to 344° C. The data showed that maximum flame speed increased with temperature at an increasing rate. The percentage change in flame speed with change in initial temperature for the three fuels followed the decreasing order, methane, propane, and ethylene. Empirical equations were determined for maximum flame speed as a function of initial temperature over the temperature range covered for each fuel.*

*For each fuel it was found that, with a fixed parallel-beam shadowgraph system, the ratio of flame speed based on the outer edge of the shadow cast by the flame cone to flame speed based on the inner edge of the shadow was a constant, independent of temperature or composition. The flame speed of propane-air flames was independent of tube diameter from 10 to 22 millimeters or stream-flow Reynolds number from 1500 to 2100.*

*The observed effect of temperature on flame speed for each of the fuels was reasonably well predicted by either the thermal theory as presented by Semenov or the square-root law of Tanford and Pease. The importance of active radicals in flame propagation was indicated by a simple linear relation between maximum flame speed and equilibrum radical concentrations for all three fuels. Equally good correlations resulted from using either hydrogen-atom concentration alone or a summation of effective relative concentrations of hydrogen atoms, hydroxyl radicals, and oxygen atoms and from using either flame temperatures based on a sodium D-line measurement for a room-temperature mixture or adiabatic flame temperatures.*


### INTRODUCTION

The flame speed, or normal burning velocity, of a fuel-air mixture is a fundamental property governing flame propagation, which is one of the several major processes occurring in combustion equipment for flight propulsion. Inasmuch as plots of the performance data of aircraft combustors show that the combustion efficiency is related to the combustor-inlet temperature (for example, references 1 and 2), knowledge of temperature effects on fundamental combustion properties of the fuel-air mixture is desirable. The results of some earlier investigations of the effect of initial mixture temperature on flame speed are summarized in reference 3. Previous investigators have found flame speed to be related (approximately) to initial temperature raised to powers varying from 1 to 2. In the first phase of the present investigation, the effect of initial temperature on flame speeds of propane-air mixtures was determined (reference 4). It was found that flame speed increased with initial temperature at an increasing rate and that this trend was predicted by either a thermal theory (reference 5) or a diffusion theory (references 6 and 7).

Inasmuch as the activation energy of the oxidation process is an important factor in the thermal-theory equations, it was decided to obtain flame-speed–temperature data for a gaseous fuel having an activation energy appreciably different from that of propane. Methane was selected because it has an activation energy of 51 kilocalories per gram-mole (reference 8) compared with 38 kilocalories per gram-mole for propane (reference 9, p. 437).

It was also thought that data for ethylene, which had shown anomalous behavior in other correlations (reference 10) when compared with other hydrocarbons, would be of value. The activation energy of ethylene, which is approximately 40 kilocalories per gram-mole (reference 11), is close to that of propane.

The present report contains the results of a study of the effect of initial mixture temperature on the laminar flame speeds of methane-air mixtures over the range from —132° to 342° C and of propane-air and ethylene-air mixtures over the range from —73° to 344° C. The flame speeds were computed from measurements based on the outer edge of the shadow cast by the Bunsen cone; the shadowgraphs were obtained with a parallel-beam shadowgraph system. The flame-speed values thus obtained at 25° C are compared with values obtained by other methods.

Methane, propane, and ethylene are compared on the basis of relative increase in flame speed with initial temperature. Empirical equations for flame speed as a function of initial temperatures are presented. A comparison is also made among the experimental data for each fuel and the relative effects of temperature on flame speed predicted by the thermal and diffusion theories.

[1] Supersedes NACA TN 2170, "Effect of Initial Mixture Temperature on Flame Speeds and Blow-Off Limits of Propane-Air Flames", by Gordon L. Dugger, 1950, and NACA TN 2374, "Effect of Initial Mixture Temperature on Flame Speed of Methane-Air, Propane-Air, and Ethylene-Air Mixtures", by Gordon L. Dugger, 1950.

## SYMBOLS

The following symbols are used in this report:

$A$ longitudinal cross-sectional area of cone (sq cm)
$a_0$ number of molecules of combustible per unit volume of initial mixture
$b, c$ constants in empirical equation for given fuel
$\overline{c_p}$ mean specific heat $T_0$ to $T_f$ (cal/(g)(° K))
$c_{p,f}$ specific heat at flame temperature (cal/(g)(° K))
$D_f$ diffusion coefficient at flame temperature (cm²/sec)
$D_i$ diffusion coefficient of $i^{th}$ radical at initial temperature (cm²/sec)
$D_{i,r}$ relative diffusion coefficient of $i^{th}$ radical with respect to other radicals
$D_m$ diffusion coefficient of $i^{th}$ radical at mean combustion-zone temperature (cm²/sec)
$E$ activation energy (cal/g-mole)
exp base of Napierian logarithmic system raised to power in parenthesis following exp
$h$ height of cone (cm)
$K$ constant from specific rate equation
$k_i$ specific rate constant for reaction between $i^{th}$ radical and combustible material
$l$ slant height or length of generating curve (cm)
$n$ constant exponent in empirical equation for given fuel
$n_1/n_2$ moles of reactants per moles of products from stoichiometric equation
$p_i$ mole fraction or partial pressure of $i^{th}$ radical in burned gas
$R$ gas constant (cal/(g-mole)(° K))
$S$ lateral surface area (sq cm)
$T$ absolute temperature (° K)
$T_f$ flame temperature (° K)
$T_0$ initial mixture temperature (° K)
$u$ flame speed (cm/sec)
$\lambda_f$ thermal conductivity at flame temperature (cal/(cm²) (sec)(° K/cm))
$\rho_f$ density at flame temperature (g/cm³)
$\rho_0$ density mixture at initial temperature (g/cm³)

## EXPERIMENTAL PROCEDURE

The flow system, high-temperature burner, and optical system are diagrammatically illustrated in figure 1. For low-temperature data, the same apparatus was used, except that the low-temperature burner illustrated in figure 2 was substituted for the high-temperature burner at section X–X in figure 1. The fuel and air were metered, mixed, heated (or cooled), and burned above a vertical tube.

**Fuels.**—The minimum purities claimed by the suppliers of the methane and ethylene were 99.0 and 99.5 percent, respectively. The propane had a minimum purity of 95.0 percent, the principal impurities being ethane and isobutane. Laboratory service air containing approximately 0.3 percent water by weight was used.

**Metering system.**—The fuel and air flows were metered by sets of critical-flow orifices (reference 12). For each orifice, when the upstream pressure was measured with a 100-inch mercury manometer, the ratio of highest measurable flow rate to lowest was 2:1; for a set of six orifices, the overall ratio of measurable flow rates was 64:1. The six orifices

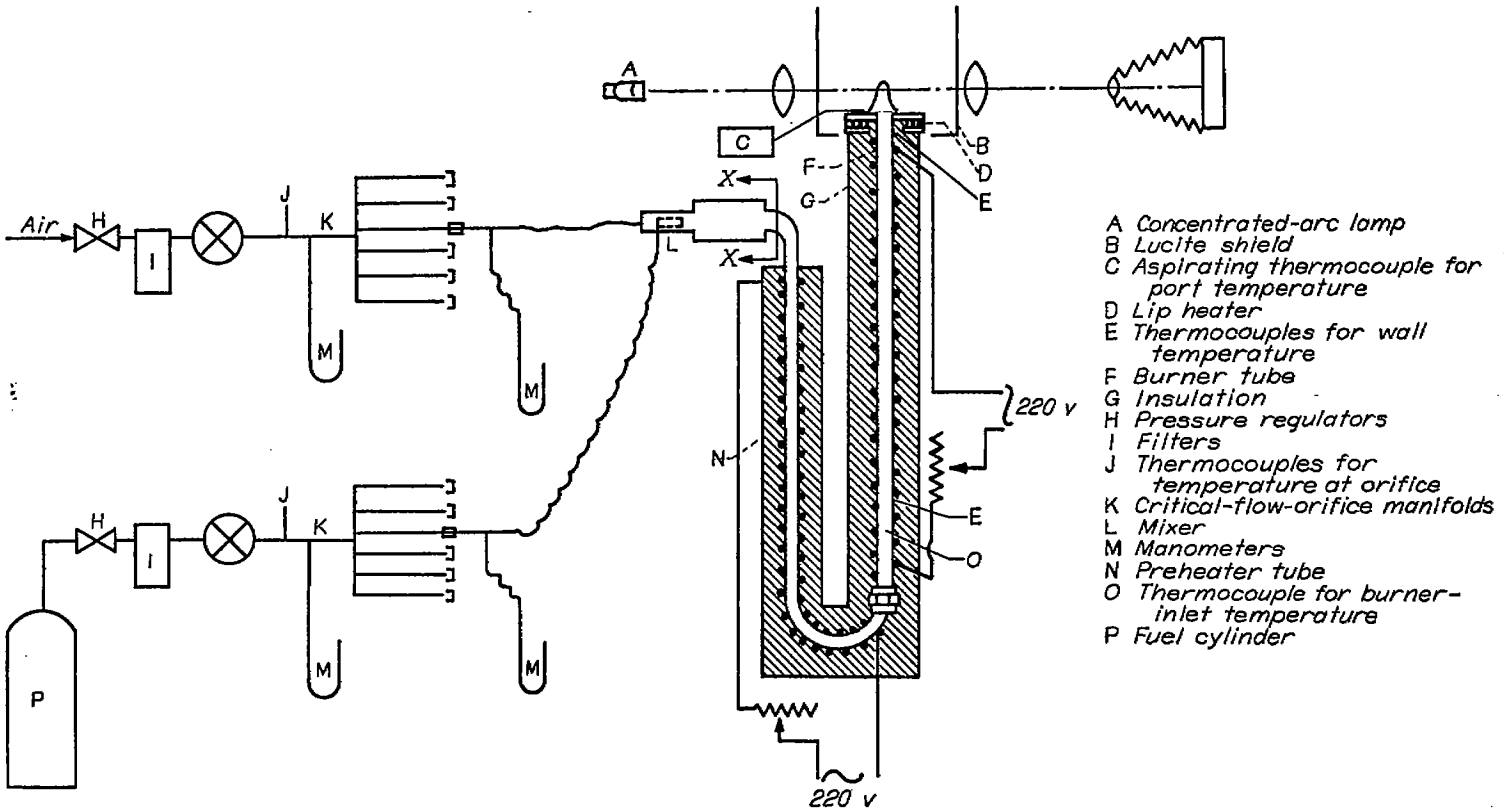


FIGURE 1.—Diagrammatic sketch of experimental apparatus, showing high-temperature burner. X–X, section at which high- and low-temperature burners are exchanged.

were mounted in parallel in a manifold, five of them being capped, while the one in use was connected by a flexible hose to the mixer. Ruby bearing-jewels of appropriate sizes were used as the orifice plates. Upstream temperatures were measured by iron-constantan thermocouples.

**High-temperature burners.**—The burners used for the data obtained at and above room temperature were straight lengths of brass tubing of the following inside diameters: for methane, 15.7 millimeters; for propane, 10.2, 15.7, and 22.2 millimeters; and for ethylene, 6.3 millimeters. Burner lengths of at least 70 diameters were used, which insured laminar flow. Each burner tube was wrapped with asbestos-covered resistance wire and insulated to permit control of the tube-wall temperature. A 76-millimeter-diameter brass collar was silver-soldered to the lip of each tube to give a flat horizontal surface above the insulation. A small resistance heater was fastened to the under side of the collar for the methane and ethylene studies; in the earlier propane studies the lip temperature was established by the heating due to the flame itself. The heater section, which consisted of a 150-centimeter length of 9.5-millimeter-inside-diameter stainless-steel tubing, was attached by a union to the base of the burner tube. The heater tube was also wrapped with resistance wire and insulated.

Temperatures were measured by iron-constantan thermocouples installed at the burner-tube inlet and at the burner-tube port for both wall and gas temperature. The thermocouple for measuring the gas temperature at the port (thermocouple C) was of the aspirating type (reference 13) and was placed directly over the center of the port between runs. The gas temperatures at the port and at the burner inlet (thermocouple O) were maintained within 10° C of each other.

**Low-temperature burner.**—For the low-temperature data, a nozzle-type burner was used in order to obtain laminar flow in a short over-all burner length, so that the whole burner assembly could be submerged in an 18-centimeter-diameter by 33-centimeter-deep Dewar vessel. The burner assembly is illustrated in figure 2.

The burner proper was made of brass and had an over-all length of 30.5 centimeters. The fuel-air mixture was fed through the inlet tube I to the manifold K, from which it entered the burner by means of 16 small holes J, equally spaced circumferentially about the base. It then passed through the straight section H and through four calming screens D, which were supported by brass rings G and sealed by neoprene O-rings F. The mixture was then accelerated by a Mache-Hebra type brass nozzle C (reference 14) and further accelerated by a small ceramic nozzle A, which was cemented to the brass nozzle.

The ceramic nozzle was added to the original brass nozzle when it was found that such an arrangement aided in stabilizing the flame. The improved stability was presumably due to the reduced thermal gradient between flame and nozzle, since stable, regularly shaped flames were obtained only after the flame had been allowed to heat the ceramic

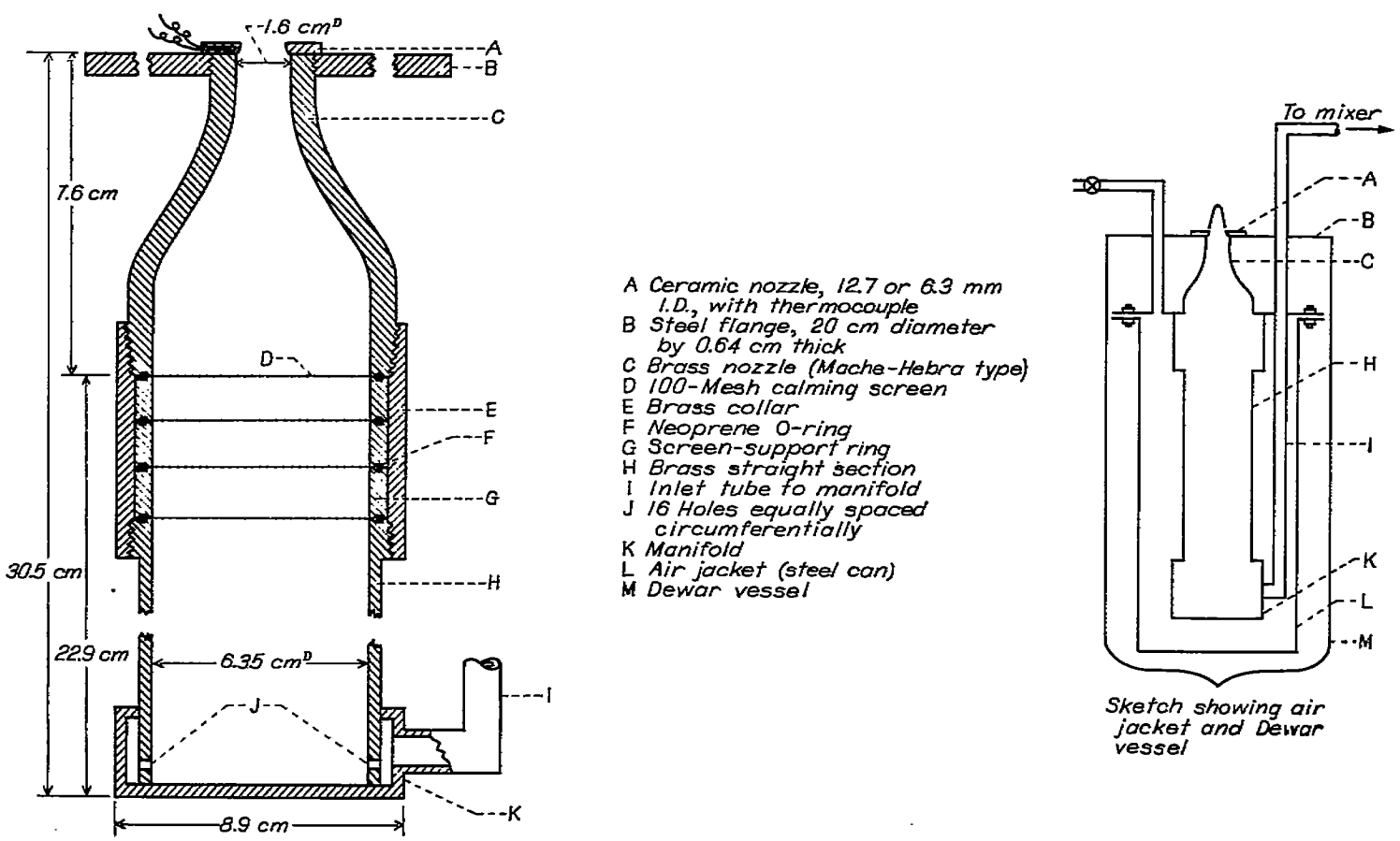


FIGURE 2.—Detail of low-temperature burner.

nozzle to a temperature 60° to 100° C higher than the gas temperature. Tests made with a propane-air mixture at room temperature indicated that this difference between the temperature of the short ceramic nozzle and the gas temperature did not appreciably affect flame speed. For methane and propane, the ceramic nozzle had a throat diameter of 12.7 millimeters; for ethylene, 6.3 millimeters. These nozzles were turned from round stock by cutting an axial hole to the desired throat diameter and then rounding the upstream edge of the hole to approximately a 1.6-millimeter radius. The nozzle disks were 3.2 millimeters thick.

In figure 3, a velocity profile is shown for the 12.7-millimeter ceramic nozzle (on the brass nozzle) for an average air-flow velocity (volumetric flow rate divided by nozzle-throat area) of 124 centimeters per second at 25° C. The profile was obtained by means of a hot-wire-anemometer

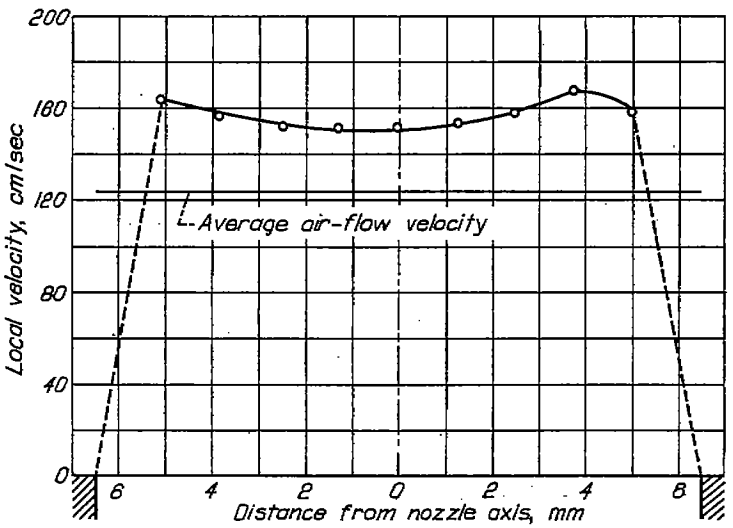


FIGURE 3.—Velocity profile above 12.7-millimeter ceramic nozzle cemented to brass nozzle. Air temperature, 25° C; Reynolds number, 1020.

probe, which was calibrated the same day by traverses of fully developed laminar flow (reference 15) in a 25-millimeter-inside-diameter tube. The calibration curve was established by assuming the local velocity at the axis of the 1-inch tube to be twice the average velocity and the average velocity to be equal to the local velocity at a distance from the tube axis equal to 0.707 times the tube radius. This condition was experimentally confirmed within ±5 percent, which is believed to be the accuracy of the measurements. The average velocity computed from the anemometer readings was 131 centimeters per second, assuming a linear velocity gradient from the outermost data points to the nozzle wall. While the central portion of the velocity profile is fairly flat, the local velocities over this portion are of the order of 20 percent higher than the average velocity (volumetric flow rate divided by nozzle-throat area). Since flame-speed values based on a local velocity, which was assumed to be equal to the average velocity, would thus have been in great error, it was decided to use the total-area method of flame-speed measurement (described hereinafter) for nozzle flames as well as tube flames. While the two-stage nozzle referred to herein is an unusual case, it is believed that an appreciable error would result from ignoring the boundary-layer effect for any small-diameter nozzle.

For the data obtained at −73° C, the burner as described was submerged in a bath of dry ice in acetone and was supported on the lip of the Dewar vessel M by the steel flange B, which was screwed onto the brass nozzle. For the data at −132° C, for which liquid nitrogen was used as the coolant, it was found necessary to jacket the lower three-quarters of the burner with air to prevent overcooling and consequent condensation of oxygen from the primary air. This jacketing was accomplished by bolting a steel can L to a flange soldered to the brass nozzle. The desired nozzle-outlet temperature was then obtained by varying the level of liquid nitrogen with respect to the top of the air jacket.

The gas temperature was measured between runs by a bare 28-gage copper-constantan thermocouple, which had a soft-solder head of approximately 1.5-millimeter diameter at the junction. It was supported in a piece of pyrex tubing with a right-angle bend such that the thermocouple leads extended downward (along the axis of the gas stream) for a distance of 6 centimeters. The wall temperature of the ceramic nozzle was measured by another copper-constantan thermocouple. For the −73° C data, it was believed that errors in the gas-temperature readings due to radiation and lead-conduction losses were of the order of ±1 percent. For the −132° C data, errors due to radiation and lead conduction when the thermocouple was placed in the nozzle throat were greater. A correction was estimated by the following method: Gas-temperature readings were taken with the junction at depths of 0.3 and 5.0 centimeters below the top surface of the ceramic nozzle. Of these two temperature readings, the 5-centimeter reading was subject to smaller lead-conduction and radiation errors because the junction was well inside the cold nozzle. With the two gas-temperature readings and the ceramic-nozzle temperature known for flow without burning, an estimate was made of the correction to be applied to the 5-centimeter reading in order to obtain the correct temperature of the gas leaving the nozzle throat (initial mixture temperature). It was assumed that the lead-conduction error was negligible; the radiation and wall-to-gas heat-transfer corrections (estimated from reference 16) totaled 5° C. The initial mixture temperature was therefore taken to be the 5-centimeter reading plus 5° C.

**Determination of flame speed.**—Shadowgraphs of the flames were made by a parallel-beam system as shown schematically in figure 1. Flame speeds were determined from the shadowgraphs by the total-area method, wherein the average normal flame speed is equal to the volume rate of flow of the unburned mixture divided by the surface area of the cone formed by the combustion zone. This surface area was determined by assuming that the flame surface can be approximated by the relation for conical surfaces of revolution; thus,

$$S=\pi A\ l/h \qquad (1)$$

A typical shadowgraph is shown in figure 4. The area $A$ was determined by measuring a magnified image of the shadow cone with a planimeter; the magnified image was obtained by tracing the outer edge of the shadow from the projected image of the shadowgraph. Because of inaccuracies in tracing and in using a planimeter, a scatter in the computed points resulted, especially for the tall slender ethylene flames. The precision at the higher temperatures was 4 percent for ethylene. This scatter was diminished by: (1) determining the average value of $A/h$ for all the computed points at a given temperature and flow rate; (2) recomputing flame-speed values for one of the points on the basis of the average $A/h$; and (3) computing the rest of the flame-speed values from the already corrected point by a ratio of cone heights according to the equation $u_2=u_1h_1/h_2$. This procedure essentially amounts to the method used in reference 17.

## RESULTS AND DISCUSSION

**Flame speeds based on outer edge of shadow.**—As indicated in references 11 and 18, the maximum density gradient is more nearly represented by the outer edge of the shadow than by the inner edge because of the manner in which the shadow of a flame cone is produced. If the locus of maximum density gradient is taken to correspond to the flame front, absolute values of flame speed should be based on the outer edge of the shadow. In order to obtain the relation between flame-speed values based on the inner edge of the shadow (which is more sharply defined) and values based on the outer edge of the shadow, a group of points was selected at each of six temperatures from room temperature to 344° C for each fuel and was computed on both bases. Each group consisted of one point representing the leanest mixture studied, one point near the composition for maximum flame speed, and one for the richest mixture studied. Plots of 18 points so selected for each fuel revealed no trends for the relating factor with respect to either mixture composition or temperature; the arithmetic mean value of the factors for all 18 points for a given fuel was therefore considered to be the best value over the ranges of composition and temperature studied. Inasmuch as the same constant factor applies for all the points for a given fuel, the relative effects of temperature on flame speed would be the same for flame speeds calculated from either the inner or the outer edge of the shadow. In the early part of the present investigation, values based on the inside edge of the shadow were used because the required measurements were more easily and precisely made on this basis.

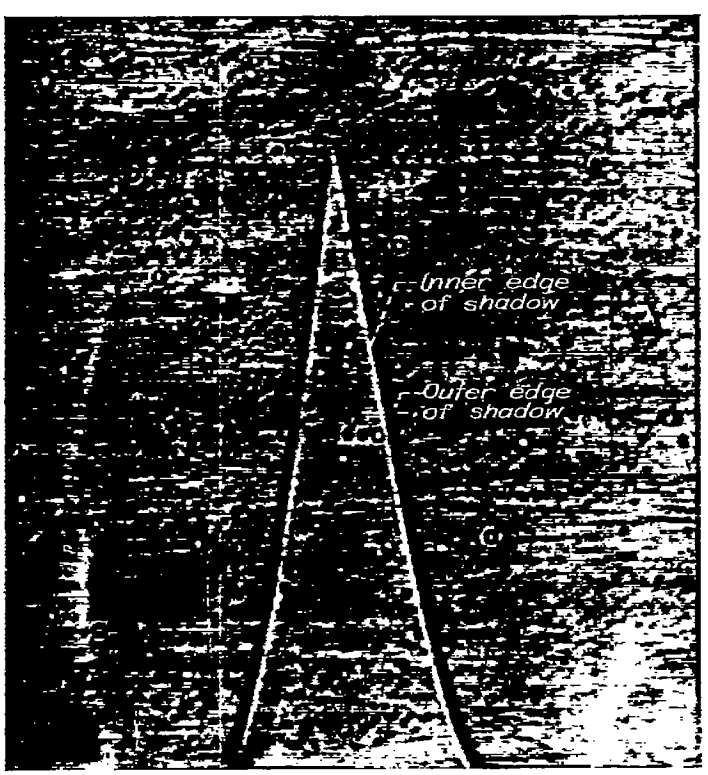


FIGURE 4.—Typical shadowgraph showing inner and outer edges of shadow cast by Bunsen cone.

The arithmetic mean values of the factors required to convert inner-edge values to outer-edge values of flame speed for the three fuels are presented in table I. The maximum flame speed at 25° C was obtained for each fuel by interpolation from figure 6 in order to compare the value with values obtained by other investigators who used shadow-cone, visible-cone, and tube measurements (references 11 and 19 to 24). The agreement among outer-edge shadow-cone, visible-cone, and tube measurements for methane and propane is good. The poorer agreement among various methods and investigators for ethylene is probably due, in part, to the greater uncertainties in measurements of the tall slender flame shapes encountered with ethylene in both Bunsen burner and tube methods.

TABLE I.—FACTORS FOR CONVERTING FLAME SPEEDS BASED ON INNER EDGE OF SHADOW TO OUTER EDGE AND COMPARISON OF 25° C VALUES WITH VISIBLE BUNSEN CONE AND TUBE MEASUREMENTS

| Fuel | Conversion factor | | Maximum flame speed at 25° C (cm/sec) | | | |
|---|---|---|---|---|---|---|
| | Mean value | Mean deviation | Inner edge | Outer edge [a] | Visible cone | Tube method [b] |
| Methane | 0.900 | 0.017 | [c] 37.8 | 34.0 | [d] 33.3 | 33.8 |
| Propane | .885 | .017 | [e] 45.4<br>[f] 45.5<br>[h] 46.6 | 40.2 | [e] 38.5<br>[g] 41.5 | 39.0 |
| Ethylene | .849 | .027 | [e] 75.4<br>[g] 74.6<br>[f] 72.0 | 64.0 | [i] 60.0 | 68.3 |

[a] Obtained from fig. 5 by interpolation.
[b] Based on total area of flame traveling at uniform velocity inside a pyrex tube (reference 18)
[c] Related to outer-edge value by conversion factor.
[d] Total-area method, inner boundary of luminous zone (reference 19).
[e] Total-area method, center of luminous zone (present investigation).
[f] Total-area value extrapolated to diametral axis of flame; value of 45.0 cm/sec obtained by stroboscopically illuminated particle method (reference 20).
[g] Based on area of upper part of shadow cone only (reference 21).
[h] Based on area of cone frustrum (reference 22).
[i] Total-area method (reference 23).
[j] Mean value of a number of measurements by angle method at different cone positions (reference 11).

In figure 5, flame speed is plotted against equivalence ratio (fraction of stoichiometric fuel-air ratio) at several initial mixture temperatures for each fuel. It is believed that no preflame reaction has occurred during the short preheating period (less than 2 sec) at these temperatures (reference 9, pp. 406, 411). The stream-flow Reynolds number was approximately 1500 for methane-air mixtures and 2000 for

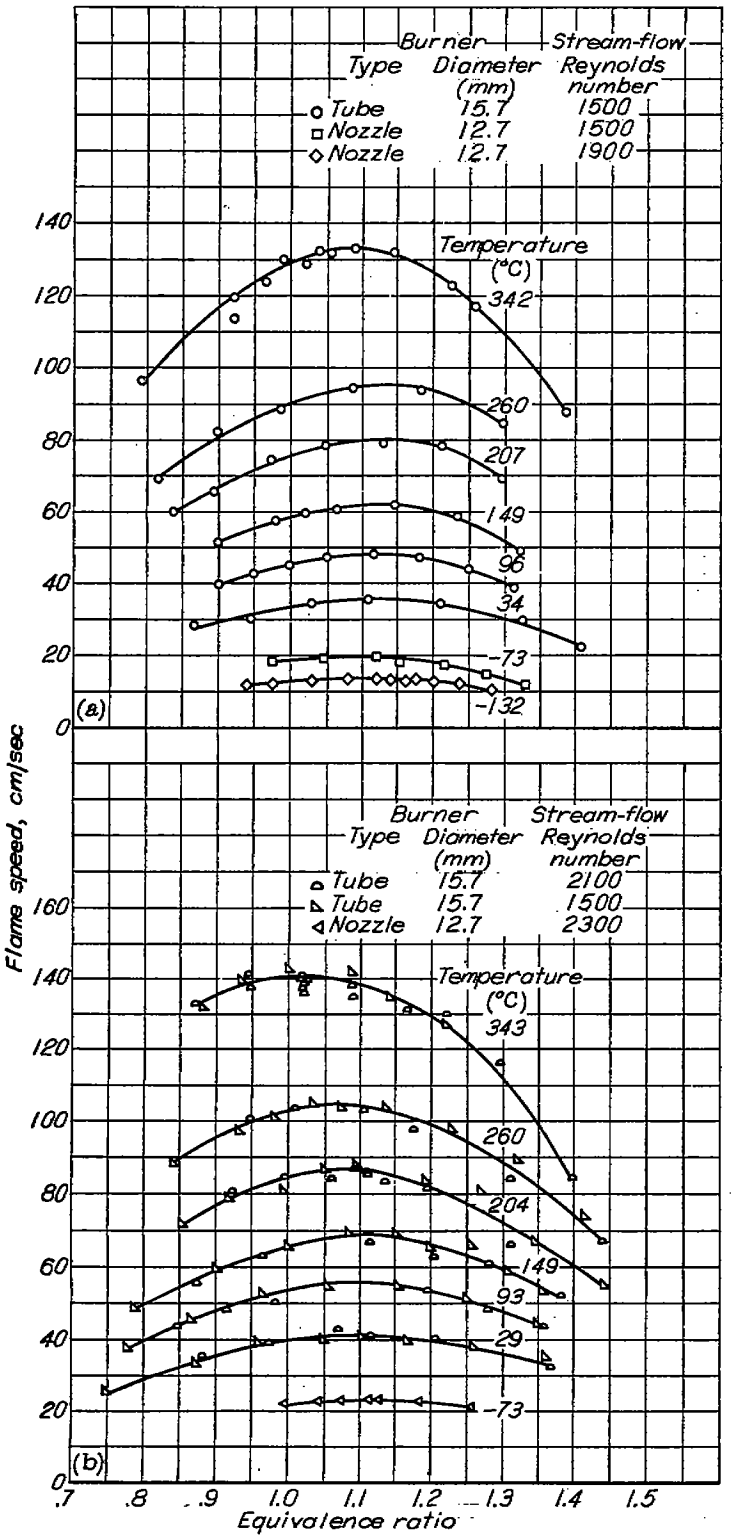


(a) Methane-air flames.
(b) Propane-air flames.

FIGURE 5.—Flame speed as function of equivalence ratio (fraction of stoichiometric fuel-air ratio) at various initial mixture temperatures.

ethylene-air mixtures. The propane-air data were taken at two Reynolds numbers, 1500 and 2100, and are plotted together, showing that Reynolds number has no appreciable effect on flame speed in this range. Preliminary propane-air data obtained by photographing the luminous flame cone above 10.2-, 15.7-, and 22.2-millimeter tubes showed the tube diameter to have little effect on maximum flame speed. A few comparative values are given in table II.

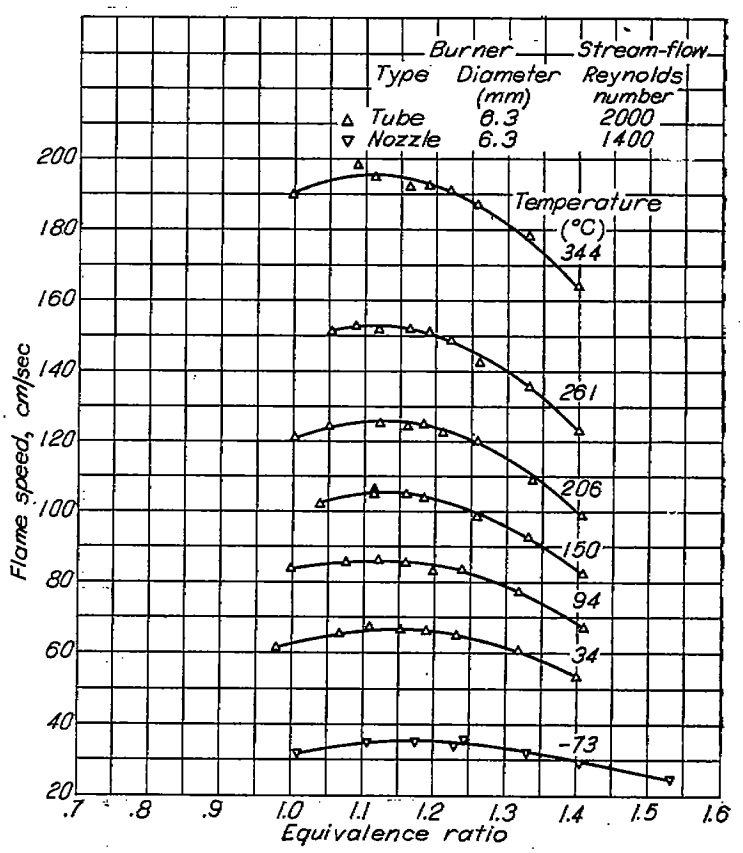


(c) Ethylene-air flames.

FIGURE 5.—Concluded. Flame speed as function of equivalence ratio (fraction of stoichiometric fuel-air ratio) at various initial mixture temperatures.

TABLE II.—COMPARISON OF PROPANE-AIR FLAME-SPEED VALUES OBTAINED WITH VARIOUS TUBE DIAMETERS

| Initial temperature (°C) | Tube diameter (mm) | Maximum flame speed (luminous cone) (cm/sec) |
|---|---|---|
| 25 | 10.2<br>15.7<br>22.2 | 38<br>39<br>39 |
| 149 | 10.2<br>15.7<br>22.2 | 69<br>68<br>71 |
| 204 | 10.2<br>15.7<br>22.2 | 83<br>81.5<br>83 |

Each of the curves in figure 5 shows that the maximum flame speed for a given temperature occurs at a mixture composition richer than stoichiometric (equivalence ratio greater than 1.0). These flame-speed maximums from figure 5 are plotted against initial mixture temperature in figure 6 to show the effect of temperature on maximum flame speed for the three fuels. It appears that the curves in figure 6 could be extrapolated to zero flame speed at zero degrees absolute.

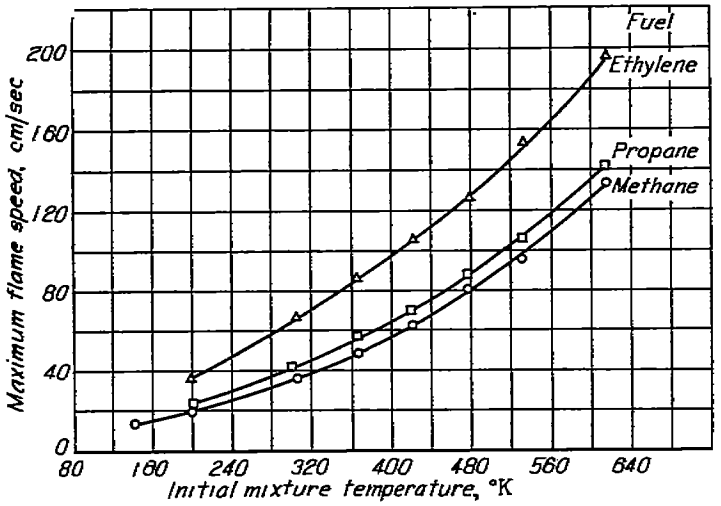


FIGURE 6.—Effect of initial mixture temperature on maximum flame speed.

It was found that the effect of initial mixture temperature ($T_0$, °K) on maximum flame speed ($u$, cm/sec) could be represented by empirical equations of the type

$$u=b+cT_0^n$$

where $b$, $c$, and $n$ are constants for a given fuel. The equations, which were determined by picking an integer for $b$ which gave a straight line on a logarithmic plot of $(u-b)$ against $T_0$ and then determining $c$ and $n$ by the method of least squares, are:

For methane at $T_0=141°$ to $615°$ K,

$$u=8+0.000160\ T_0^{2.11}$$

for propane at $T_0=200°$ to $616°$ K,

$$u=10+0.000342\ T_0^{2.00}$$

and for ethylene at $T_0=200°$ to $617°$ K,

$$u=10+0.00259\ T_0^{1.74}$$

The logarithmic plots of the equations together with the data points are presented in figure 7.

In figure 8, the percentage increase in maximum flame speed, based on the interpolated value of flame speed at 25° C, is plotted against temperature. The flame speeds of these three fuels are again seen to be affected by temperature in the decreasing order: methane, propane, and ethylene.

**Comparison of experimental data with relative values predicted by theoretical equations.**—Two proposed mechaisms for the propagation of flame are considered: One is based primarily on the conduction of heat from the combustion zone into the unburned gases and the other is based on the diffusion of active radicals from the combustion zone into the unburned gases. Both these theories are used to predict the relative effect of temperature on flame speed.

It has been pointed out that early heat theories (for example, reference 9, p. 113, and reference 5), which assumed that (a) reaction begins at the self-ignition temperature, and that (b) the reaction rate is constant between the self-ignition temperature and the flame temperature, are inadequate. The concept of ignition temperature has no meaning apart from an autoignition experiment, which requires a certain induction period. Actually, reaction rate continuously increases with temperature because it is a function of $\exp(-E/RT)$.

Semenov (reference 5) derived an approximate equation that involves only the initial mixture temperature, the flame temperature, and the physical properties at these temperatures. If the controlling step is a monomolecular reaction, the appropriate final equation is

$$u=\sqrt{\frac{2\lambda_f K c_{p,f}}{\rho_0 \overline{c_p}^2}\left(\frac{T_0}{T_f}\right)\left(\frac{\lambda}{c_p\rho D}\right)_f\left(\frac{n_1}{n_2}\right)\left(\frac{RT_f^2}{E}\right)^2\frac{\exp(-E/RT_f)}{(T_f-T_0)^2}} \tag{2}$$

and for a bimolecular reaction, the final equation is

$$u=\sqrt{\frac{2\lambda_f K a_0 c_{p,f}^2}{\rho_0 \overline{c_p}^3}\left(\frac{T_0}{T_f}\right)^2\left(\frac{\lambda}{c_p\rho D}\right)_f^2\left(\frac{n_1}{n_2}\right)^2\left(\frac{RT_f^2}{E}\right)^3\frac{\exp(-E/RT_f)}{(T_f-T_0)^3}} \tag{3}$$

Equations (2) and (3) take into account the cases where (a) specific heat and thermal conductivity vary with temperature, (b) the number of molecules changes during reaction, and (c) the diffusion coefficient $D_f$ does not equal the coefficient of temperature conductivity $(\lambda/c_p\rho)_f$. Case (c)

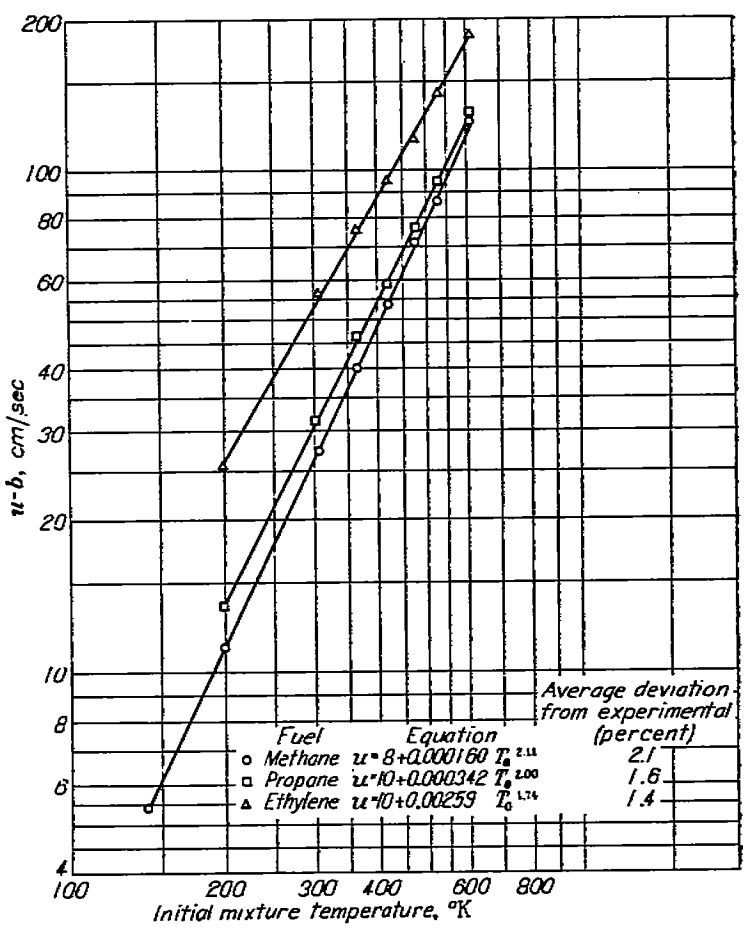


FIGURE 7.—Empirical equations for maximum flame speed as function of initial mixture temperature.

means that although the sum of the thermal and chemical energies will be the same for the over-all process, the sum of the energies will vary within the combustion zone. For example, if $D_f > (\lambda/c_p\rho)_f$, the thermal energy supplied by heat conduction upstream of the flame zone will be less than the chemical energy conducted away by diffusion. Thus, diffusion enters only as it affects the energy balance.

By elimination from equations (2) and (3) of the terms independent of temperature, by the substitution, as approximate relations for the temperature-dependent terms, of those relations determined for air, and by combining terms, the monomolecular equation can be reduced to the form

$$u \propto \sqrt{T_0^2 T_f^{3.89} \frac{\exp(-E/RT_f)}{(T_f - T_0)^2}} \tag{4}$$

and the bimolecular equation may be reduced to the form

$$u \propto \sqrt{T_0^2 T_f^{4.9} \frac{\exp(-E/RT_f)}{(T_f - T_0)^3}} \tag{5}$$

(physical properties for air were estimated from reference 16, pp. 391–411 and related to temperature as follows: $\lambda \propto T^{0.84}$; $c_{p,f} \propto T^{0.09}$; $\overline{c_p} \propto T^{0.09}$; $D \propto \mu/\rho \propto T^{1.67}$, where $\mu$ is viscosity; $\rho \propto T^{-1}$; and $a_0 \propto T^{-1}$.) These reduced forms of the equations may be used to estimate the relative effect of temperature on flame speed (thermal theory) for hydrocarbons burning with air, provided that the relations between the physical properties and the temperature for the mixture are reasonably near those for air.

A diffusion mechanism of flame propagation may also be considered for the prediction of the effect of temperature on flame speed. Tanford and Pease (references 6 and 7) have proposed that the rate of diffusion of hydrogen atoms upstream of the flame front determines the rate of flame propagation. This concept, generalized to include other radicals, which might be important for other systems, is expressed by

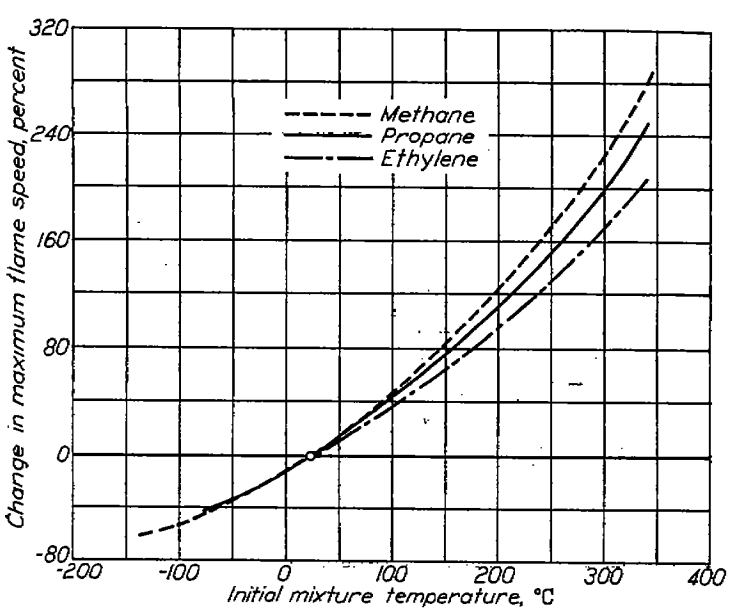


FIGURE 8.—Percentage change of maximum flame speed (based on 25° C) with initial mixture temperature.

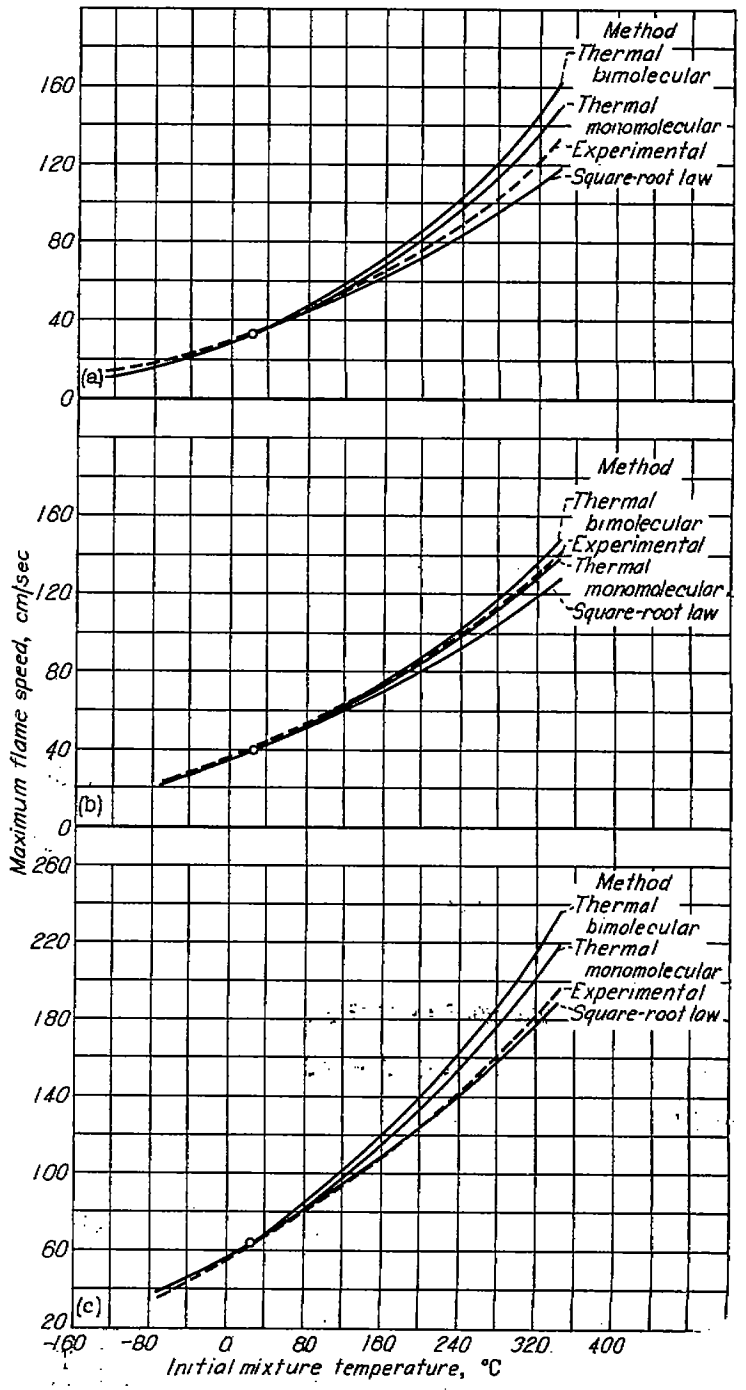


(a) Methane-air flames.
(b) Propane-air flames.
(c) Ethylene-air flames.

FIGURE 9.—Effect of initial mixture temperature on maximum flame speed. Comparison of theoretically predicted curves (based on 25° C) with experimental results.

what has been called the square-root law of burning velocity (reference 7):

$$u = \sqrt{\sum_i p_i D_i k_i L \frac{Q'}{QB_i}} \tag{6}$$

As a first approximation, it may be assumed that only $D_i$, $L$, and $p_i$ are appreciably temperature-dependent. In obtaining the temperature dependence of $D_i$, it is necessary to revert to the derivation of equation (5) (reference 6) where $D_i$ was substituted for $D_m$, the diffusion coefficient at the mean combustion-zone temperature $T_m$, by the relation

$$D_i = \frac{T_0^2}{T_m^2} D_m = \frac{T_0^2}{(0.7\,T_f)^2} D_m$$

where $T_m$ was assumed to be 0.7 $T_f$. Now if $D_m$ is assumed proportional to $T_m^{1.67}$ (the exponent which was used in equations (4) and (5)), it follows that

$$D_i \propto \frac{T_0^2}{(0.7\,T_f)^2}(0.7\,T_f)^{1.67} \propto \frac{T_0^2}{T_f^{0.33}}$$

Since $L \propto T_m^{-1} \propto T_f^{-1}$ and $\sum p_i D_i \propto \sum p_i D_{i,r} \frac{T_0^2}{T_f^{0.33}}$, where $D_{i,r}$ is the relative diffusion coefficient of the radical with respect to the other radicals, the temperature dependence of flame speed predicted by equation (6) is

$$u \propto \sqrt{\left(\sum_i p_i D_{i,r}\right) \frac{T_0^2}{T_f^{1.33}}} \qquad (7)$$

Comparisons of the relative effects of initial temperature on maximum flame speed as predicted by the reduced equations (4), (5), and (7) for methane, propane, and ethylene are presented in figure 9. The values used in plotting the curves in figure 9 (and fig. 10, discussed later) are presented in table III. The flame temperatures used in figure 9 were based on sodium D-line measurements of flame temperatures of mixtures at room temperature (reference 25). The changes in flame temperature with initial temperature were assumed to be the same as for the theoretical adiabatic flame temperature (reference 26); that is, the difference between computed adiabatic flame temperature and sodium D-line temperature was taken to be constant for a given mixture. The equilibrium radical concentrations were computed by the graphical method of reference 27.

From figure 9 and table III it may be seen that both the thermal-theory equations and the square-root law predicted (relative to the 25° C values) flame speeds within approximately 20 percent for the initial temperatures and gases studied. The comparative agreement between the different theoretical curves and the experimental curve varies for the three fuels. In general, for elevated temperatures the thermal-theory curves are high and the square-root-law curves are low; whereas, for low temperatures, the values predicted by the two theories are substantially the same.

It must be emphasized that even qualitative observations regarding the ability of one or the other of the theories to predict the effect of initial temperature on flame speed are subject to the assumptions made in deriving both the original equations and the reduced forms and to the choices of values for flame temperatures and activation energies. The effects of using different values of $T_f$ and $E$ may be illustrated by the case of propane at an initial mixture temperature of 343° C. In table III the flame-speed values predicted by the thermal-monomolecular, thermal-bimolecular, and square-root-law equations are listed as 139.0, 150.8, and 126.9 centimeters per second, respectively; whereas,

(1) Using the adiabatic flame temperatures rather than the temperatures based on the sodium D-line measurement resulted in predicted values of 137.7, 149.1, and 148.0 centimeters per second, respectively.

(2) Using $E$=25,000 instead of 38,000 calories per gram-mole resulted in predicted values of 125.6, 136.3, and 126.9 centimeters per second, respectively.

(3) Combining items (1) and (2) by using adiabatic flame temperatures and $E$=25,000 calories per gram-mole resulted in predicted values of 124.6, 135.3, and 148 centimeters per second, respectively.

TABLE III.—PREDICTED RELATIVE FLAME SPEEDS

| Fuel | Equivalence ratio [a] | Activation energy $\left(\frac{\text{kcal}}{\text{g-mole}}\right)$ (Thermal theory) | Initial temperature (° C) | Flame temperature (° K) | | Equilibrium radical pressure (total pressure of 1 atm) (atm) [b] | | | | Predicted maximum flame speed, relative to max. flame speed at 25° C (cm/sec) | | | Experimental flame speed (cm/sec) |
|---|---|---|---|---|---|---|---|---|---|---|---|---|---|
| | | | | Theoretical adiabatic [c] | Based on sodium D-line [d] | $p_H$ (adiabatic) | $p_H$ (sodium D-line) | $p_{OH}$ (sodium D-line) | $p_O$ (sodium D-line) | Thermal monomolecular [e] | Thermal bimolecular [f] | Square-root-law [g] | |
| Methane | 1.22 (10.3 vol. percent) | [h] 51 | −132 | 2053 | 2008 | $0.270\times10^{-3}$ | $0.293\times10^{-3}$ | $0.282\times10^{-3}$ | $0.003\times10^{-6}$ | 10.5 | 10.1 | 11.9 | 13.4 |
| | | | −73 | 2099 | 2045 | .340 | .255 | .407 | .005 | 17.5 | 17.1 | 18.8 | 19.2 |
| | | | 25 | 2153 | [i] 2108 | .520 | .395 | .635 | .013 | 34.0 | 34.0 | 34.0 | [i] 34.0 |
| | | | 34 | 2159 | 2114 | .538 | .408 | .665 | .014 | 35.9 | 36.0 | 35.5 | 35.5 |
| | | | 94 | 2197 | 2152 | .670 | .517 | .890 | .023 | 50.0 | 50.9 | 47.3 | 48.0 |
| | | | 150 | 2231 | 2186 | .810 | .630 | 1.13 | .036 | 66.0 | 68.2 | 60.0 | 62.0 |
| | | | 206 | 2266 | 2221 | .980 | .770 | 1.45 | .057 | 85.6 | 89.7 | 74.6 | 80.0 |
| | | | 261 | 2293 | 2253 | 1.16 | .915 | 1.80 | .084 | 107.7 | 114.5 | 90.5 | 95.0 |
| | | | 344 | 2345 | 2300 | 1.48 | 1.17 | 2.44 | .141 | 148.2 | 160.9 | 118.3 | 133.0 |
| Propane | 1.049 (4.2 vol. percent) | [h] 38 | −73 | 2204 | 2149 | .460 | .299 | 1.17 | .052 | 22.8 | 22.2 | 23.0 | 23.5 |
| | | | 25 | 2253 | 2193 | .590 | .420 | 1.62 | .086 | 40.2 | 40.2 | 40.2 | [i] 40.2 |
| | | | 29 | 2255 | 2200 | .607 | .432 | 1.65 | .088 | 41.3 | 41.3 | 41.1 | 41.5 |
| | | | 93 | 2288 | 2233 | .700 | .525 | 2.00 | .124 | 55.5 | 56.4 | 54.4 | 56.4 |
| | | | 149 | 2317 | 2262 | .880 | .627 | 2.38 | .169 | 70.2 | 72.5 | 67.8 | 69.2 |
| | | | 204 | 2345 | 2290 | 1.00 | .737 | 2.80 | .228 | 86.8 | 91.0 | 82.6 | 87.0 |
| | | | 260 | 2371 | 2316 | 1.16 | .855 | 3.26 | .300 | 105.7 | 112.3 | 98.7 | 105.0 |
| | | | 343 | 2412 | 2357 | 1.43 | 1.07 | 4.10 | .469 | 139.0 | 150.8 | 126.9 | 141.2 |
| Ethylene | 1.165 (7.5 vol. percent) | [j] 40 | −73 | 2302 | 2198 | 1.13 | .629 | .94 | .035 | 35.8 | 35.0 | 37.5 | 35.5 |
| | | | 25 | 2352 | 2248 | 1.46 | .855 | 1.28 | .061 | 64.0 | 64.0 | 64.0 | [i] 64.0 |
| | | | 34 | 2356 | 2252 | 1.48 | .875 | 1.32 | .064 | 66.9 | 67.0 | 66.8 | 66.5 |
| | | | 94 | 2386 | 2282 | 1.72 | 1.02 | 1.64 | .093 | 88.3 | 89.8 | 86.0 | 86.0 |
| | | | 150 | 2413 | 2309 | 1.96 | 1.17 | 1.95 | .126 | 111.3 | 114.8 | 106.1 | 105.7 |
| | | | 206 | 2440 | 2336 | 2.23 | 1.35 | 2.33 | .171 | 137.6 | 144.0 | 128.0 | 126.0 |
| | | | 261 | 2465 | 2361 | 2.50 | 1.53 | 2.70 | .222 | 166.1 | 176.1 | 151.0 | 153.0 |
| | | | 344 | 2504 | 2400 | 3.00 | 1.83 | 3.39 | .331 | 218.2 | 236.8 | 189.8 | 196.0 |

[a] Fraction of stoichiometric fuel-air ratio at which maximum flame speed occurred.
[b] Computed by method of reference 26.
[c] Computed by method of reference 25.
[d] Computed by subtracting from adiabatic flame temperature a constant equal to difference between adiabatic and sodium D-line values (reference 24) at 25° C.
[e] Computed from equation (4).
[f] Computed from equation (5).
[g] Computed from equation (7).
[h] Reference 8.
[i] Computed using same difference between adiabatic and sodium D-line values as was found for 10.0-percent methane.
[j] Obtained from fig. 6 by interpolation.
[k] Reference 9, p. 437.
[l] Reference 11.

The difference between adiabatic and sodium D-line flame temperatures can be seen to increase from methane to propane to ethylene. It might be argued that since this difference increased from fuel to fuel in the same order as the sodium D-line flame temperatures increased at the reference initial temperature of 25° C, the difference should not be constant for a given fuel, but should increase as the flame temperature increases. In other words, the sodium D-line temperature of 2400° K for ethylene at an initial temperature of 344° C might be too high. On this premise, the predictions of equations (4), (5), and (7) were recomputed for ethylene for a flame temperature of 2350° K at the initial temperature of 344° C and were found to give predicted flame-speed values of 196.6, 214, and 170.6 centimeters per second, respectively. These predicted values are well within 20 percent of the experimental value of 196.0 and compare with the predicted values of 218.2, 236.8, and 189.8 centimeters per second listed in table III.

It is assumed herein that the variation of $B_i$, a term that appears in the square-root law to allow for radical recombination, with initial temperature is relatively small and would not appreciably affect the curves in figure 6. The temperature dependence of $k_i$, the rate constant which appears in the square-root law for interaction between the $i^{th}$ radical and the combustible material, has been neglected. Constant values of $k_i$ were used for hydrogen, carbon monoxide, and methane flames in reference 7 where the variations in flame temperature are of the same order of magnitude as those considered herein. If the temperature dependence of $k_i$ is represented by $\exp(-E/RT_f)$, the temperature effect on flame speed due to $k_i$ will be small, provided that the activation energy for the radical-hydrocarbon reaction is small. For example, with an activation energy of 7 kilocalories per gram-mole (reference 7), the relative flame speeds predicted by the square-root law for methane, propane, and ethylene would be raised approximately 8, 6, and 5 percent, respectively, at an initial temperature of 344° C and less at lower initial temperatures.

The relative merits of the theories could be better assessed if reliable data for the effect of pressure on flame speed were available. The thermal-theory equations presented in reference 5 predict that for a monomolecular reaction, the flame speed should be inversely proportional to the square root of the absolute pressure; whereas, for a bimolecular reaction, the flame speed should be independent of pressure. The square-root law predicts that flame speed should vary approximately inversely as the fourth root of the pressure (reference 7). If one of the theories could be shown to be the more consistent in predicting both pressure and temperature effects, it would be strengthened considerably. Although some pressure data exist with which this precept might be tested, conflicting trends for the variation of flame speed with pressure for a given fuel have been reported by different investigators, or by the same investigator using different experimental methods, which indicates that some of these data were influenced by the experimental apparatus. For example, in reference 28 the flame speed of ethylene measured by a Bunsen burner method was found to be inversely proportional to the fourth root of pressure; whereas, according to reference 29, the flame speed of ethylene measured by a soap-bubble method was found by the same investigator to be independent of pressure.

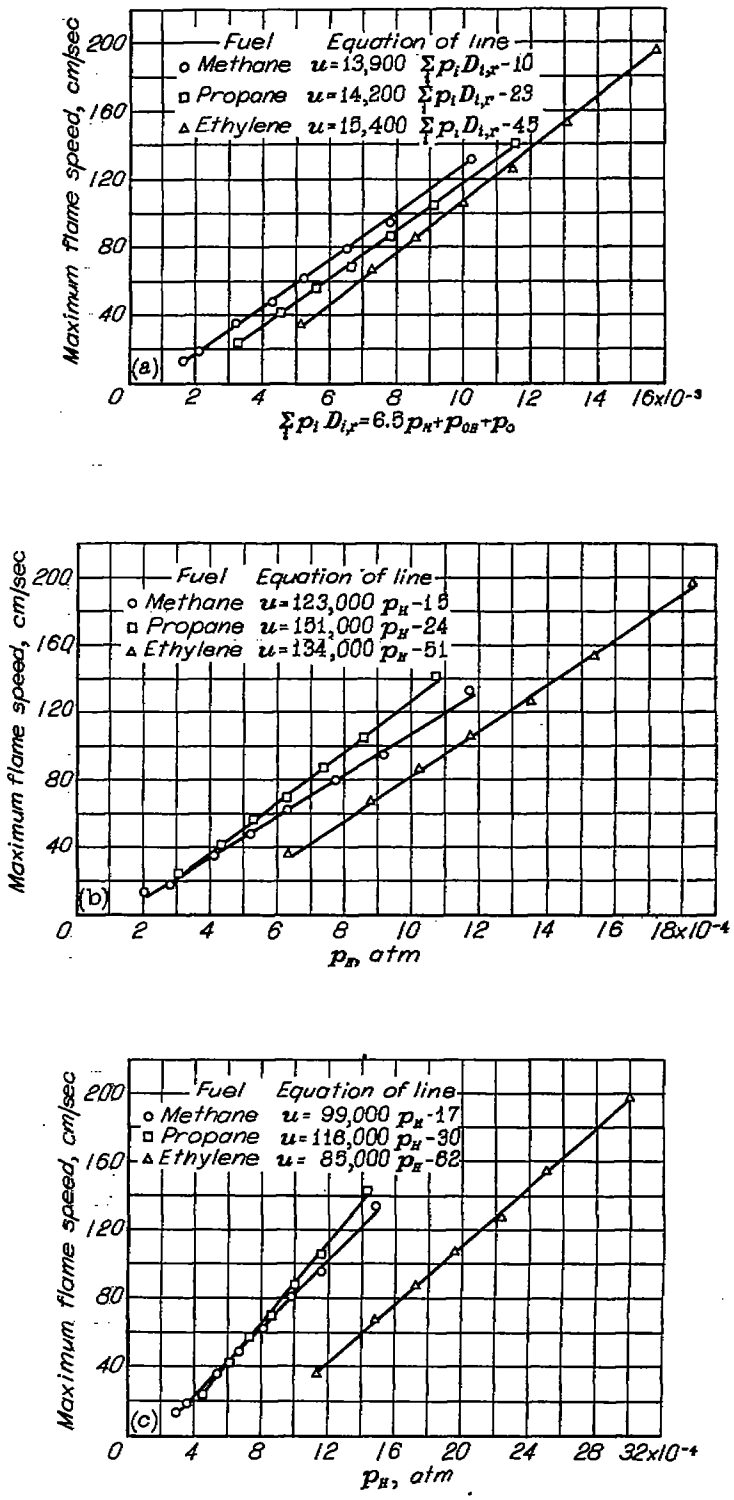


(a) Summation of effective relative radical pressures at flame temperatures based on sodium D-line measurements.

(b) Hydrogen-atom concentration at flame temperature based on sodium D-line measurement.

(c) Hydrogen-atom concentration at adiabatic flame temperature.

FIGURE 10.—Correlations between maximum flame speed and calculated equilibrium radical concentration.

**Correlation of flame speeds with active-radical concentrations.**—A correlation between flame speed and $\sum_i p_i D_{i,r}$ for ethylene-air mixtures of various compositions at room temperature is found in reference 11. In figure 10 (a), the maximum flame speeds from figure 4 are plotted against $\sum_i p_i D_{i,r}$ computed from radical pressures at temperatures based on sodium D-line measurements in table I; in figure 10 (b), maximum flame speeds are plotted against computed hydrogen-atom concentrations at these same temperatures; and in figure 10 (c) maximum flame speeds are plotted against hydrogen-atom concentrations at theoretical adiabatic flame temperatures. In all cases, straight-line correlations are obtained. The equations of these straight lines are given on the figures.

The curves of figure 10 (c) indicate that, at least for the three fuels studied, the maximum flame speed of a gaseous fuel may be accurately determined over a considerable range of initial mixture temperature when the experimental values at two temperatures are known and sufficient data exist to compute the adiabatic flame temperatures and, hence, the equilibrium hydrogen-atom concentrations. It is recognized that the slopes of the correlation lines in figure 10 are much steeper than those shown in the correlations in reference 10. In considering this difference, it must be remembered that, for a given correlation line in figure 10, initial mixture temperature varied while equivalence ratio (composition) and fuel type were fixed; whereas in reference 10 fuel type varied while initial temperature was fixed and equivalence ratios were essentially the same. The data reported herein indicate that flame speeds for a given fuel vary from fivefold to tenfold over the range of temperatures studied, whereas in reference 10 a range of only twofold was covered in the flame speeds for different fuels at the same initial temperature. However, the flame-temperature and the radical-concentration ranges are of the same order in both studies. The reasons for the difference in slope may, in part, be attributed to the temperature dependency of the other factors, such as reaction rate, in the original Tanford and Pease equation (reference 6). Inasmuch as the present data are self-consistent, it is valid to use these data to predict the effect of initial mixture temperature on maximum flame speed.

## SUMMARY OF RESULTS

An investigation of the effect of initial mixture temperature on the laminar flame speeds of methane-air, propane-air, and ethylene-air mixtures gave the following results:

1. The flame speeds of methane, propane, and ethylene increased with initial mixture temperature at an increasing rate. The percentage change in flame speed with change in initial temperature for the three fuels followed the decreasing order, methane, propane, and ethylene. Empirical equations for maximum flame speed $u$ (cm/sec; based on the outer edge of the shadow cast by the cone) for use in the temperature ranges indicated were:

For methane, at an initial mixture temperature $T_0$ of 141° to 615° K,

$$u=8+0.000160\ T_0^{2.11}$$

for propane, for $T_0$=200° to 616° K,

$$u=10+0.000342\ T_0^{2.00}$$

and for ethylene, for $T_0$=200° to 617° K,

$$u=10+0.00259\ T_0^{1.74}$$

2. Flame-speed values based on the outer edge of the shadow cast by the Bunsen cone (total-area method) were close to those based on both visible Bunsen cone measurements and tube measurements for methane and propane, but the variation in values obtained by the three methods was greater for ethylene. For each fuel, a factor was determined to allow conversion of values based on the inner edge of the shadow to values based on the outer edge of the shadow; the conversion factors were constant with respect to both temperature and composition, within the accuracy of the measurements based on the outer edge of the shadow. The flame speed of propane-air flames was independent of tube diameter from 10 to 22 millimeters and of values of stream-flow Reynolds number from 1500 to 2100.

3. Both the thermal-theory equations presented by Semenov and the square-root law of Tanford and Pease (diffusion theory) were used to predict relative flame speeds within approximately 20 percent for the temperatures and gases studied. The comparative agreement between the values predicted by the different theoretical equations and the experimental value varied for the three fuels. In general, for elevated temperatures, the thermal-theory values were high and the square-root-law values were low; whereas, for low temperatures, the values predicted by the two theories were substantially the same. However, even qualitative observations regarding the relative merits of the two theories are subject to the assumptions made and the flame temperatures and activation energies used.

4. Very good straight-line correlations between maximum flame speed and either the hydrogen-atom concentration alone or the summation of the effective relative concentrations of hydrogen atoms, hydroxyl radicals, and oxygen atoms were found for the three fuels. Equally good correlations were obtained either from flame temperatures based on sodium D-line measurements or from adiabatic flame temperatures. The slopes of the correlation lines were steeper than those reported elsewhere in investigations of the effects of mixture composition and fuel type on flame speed. Further experimental and theoretical investigation may show why the slopes were different and give better insight into the mechanisms involved in flame propagation.

Lewis Flight Propulsion Laboratory
National Advisory Committee for Aeronautics
Cleveland, Ohio, *August 20, 1951*

## REFERENCES


1. Childs, J. Howard, McCafferty, Richard J., and Surine, Oakley W.: Effect of Combustor-Inlet Conditions on Performance of an Annular Turbojet Combustor. NACA Rep. 881, 1947. (Formerly NACA TN 1357.)
2. Mullen, James W., II, Fenn, John B., and Garmon, Roland C.: Burners for Supersonic Ram-Jets. Ind. and Eng. Chem., vol. 43, no. 1, Jan. 1951, pp. 195–211.
3. Keller, J. D.: Flame Speed as Affected by Preheating of Gaseous Fuels. Industrial Heating, vol. XVII, no. 5, May 1950, pp. 780–786.
4. Dugger, Gordon L.: Effect of Initial Mixture Temperature on Flame Speeds and Blow-Off Limits of Propane—Air Flames. NACA TN 2170, 1950.
5. Semenov, N. N.: Thermal Theory of Combustion and Explosion. III. Theory of Normal Flame Propagation. NACA TM 1026, 1942.
6. Tanford, Charles, and Pease, Robert N.: Theory of Burning Velocity. II. The Square Root Law for Burning Velocity. Jour. Chem. Phys., vol. 15, no. 12, Dec. 1947, pp. 861–865
7. Tanford, Charles: The Role of Free Atoms and Radicals in Burner Flames. Third Symposium on Combustion and Flame and Explosion Phenomena, The Williams & Wilkins Co. (Baltimore), 1949, pp. 140–146.
8. Chamberlain, G. H. N., et Walsh, A. D.: L'oxydation lente de l'éther diisopropylique dans l'intervalle de températures 360°–460°C. Revue de L'Institut Francais du Pétrole et Annales des Combustibles Liquides, Vol. IV, No. 7, Juillet 1949, P. 315.
9. Jost, Wilhelm: Explosion and Combustion Processes in Gases. McGraw-Hill Book Co., Inc., 1946.
10. Simon, Dorothy Martin: Flame Propagation. III. Theoretical Consideration of the Burning Velocities of Hydrocarbons. Jour. Am. Chem. Soc., vol. 73, no. 1, Jan. 1951, pp. 422–425.
11. Linnett, J. W., and Hoare, M. F.: Burning Velocities in Ethylene-Air-Nitrogen Mixtures. Third Symposium on Combustion and Flame and Explosion Phenomena, The Williams & Wilkins Co. (Baltimore), 1949, pp. 195–203; discussion by Kurt Wohl, pp. 203–204.
12. Andersen, J. W., and Friedman, R.: An Accurate Gas Metering System for Laminar Flow Studies. Rev. Sci. Instruments, vol. 20, no. 1, Jan. 1949, pp. 61–66.
13. Anon.: Temperature. Its Measurement and Control in Science and Industry. Reinhold Pub. Corp., 1941, pp. 847–854.
14. Mache, Heinrich, und Hebra, Alexius: Zur Messung der Verbrennungsgeschwindigkeit explosiver Gasgemische. Akademie der Wissenschaften in Wien, Math.-naturw. Klasse. Sitzungsberichte. Vol. 150, Abt. IIa, 1941, S. 157–174.
15. Dodge, Russel. A., and Thompson, Milton J.: Fluid Mechanics. McGraw-Hill Book Co., Inc., 1st ed., 1937, pp. 171–175.
16. McAdams, William H.: Heat Transmission. McGraw-Hill Book Co., Inc., 2d ed., 1942.
17. Bollinger, Lowell M., and Williams, David T.: Effect of Reynolds Number in Turbulent-Flow Range on Flame Speeds of Bunsen Burner Flames. NACA Rep. 932, 1949. (Formerly NACA TN 1707.)
18. Grove, J. R., Hoare, M. F., and Linnett, J. W.: The Shadow Cast by a Bunsen Flame, Its Production and Usefulness. Trans. Faraday Soc. (London), vol. 46, pt. 9, Sept. 1950, pp. 745–755.
19. Gerstein, Melvin, Levine, Oscar, and Wong, Edgar L.: Fundamental Flame Velocities of Pure Hydrocarbons. I-Alkanes, Alkenes, Alkynes, Benzene, and Cyclohexane. NACA RM E50G24, 1950.
20. Wohl, Kurt, and Kapp, Numer M.: Flame Stability at Variable Pressures. Meteor Rep. UAC-42, Res. Dept., United Aircraft Corp., Oct. 1949. (Proj. METEOR, BuOrd. Contract Nord 9845 with M. I. T.).
21. Andersen, J. W., and Fein, R. S.: Measurement and Correlation of Burning Velocities of Propane-Air Flames. Rep. CM-552, Dept. Chem., Naval Res. Lab., Univ. Wisconsin, July 20, 1949. (BuOrd Contract Nord 9938, Task WIS-1-G.)
22. Calcote, Hartwell F., Barnett, Charles M., and Irby, Moreland R.: The Burning Velocity of Various Compounds by the Bunsen Burner Method. Paper presented at 116th Meeting Am. Chem. Soc. (Atlantic City, N. J.), Sept. 18–23, 1949. (See Abstracts of Papers 116th Meeting of Am. Chem. Soc., p. 38P.)
23. Harris, Margaret E., Grumer, Joseph, von Elbe, Guenther, and Lewis, Bernard: Burning Velocities, Quenching, and Stability Data on Nonturbulent Flames of Methane and Propane with Oxygen and Nitrogen. Third Symposium on Combustion and Flame and Explosion Phenomena, The Williams & Wilkins Co. (Baltimore), 1949, pp. 80–89.
24. Culshaw, G. W., and Garside, J. E.: A Study of Burning Velocity Third Symposium on Combustion and Flame and Explosion Phenomena, The Williams & Wilkins Co. (Baltimore), 1949, pp. 204–209.
25. Perry, John H.: Chemical Engineers' Handbook. McGraw-Hill Book Co., Inc., 2d ed., 1941, p. 2410.
26. Hottel, H. C., Williams, G. C., and Satterfied, C. N.: Thermodynamic Charts for Combustion Processes, Pt. I. John Wiley & Sons, Inc., 1949.
27. Huff, Vearl N., and Calvert, Clyde S.: Charts for the Computation of Equilibrium Composition of Chemical Reactions in the Carbon-Hydrogen-Oxygen-Nitrogen System at Temperatures from 2000° to 5000° K. NACA TN 1653, 1948.
28. Linnett, J. W., and Wheatley, P. T.: Effect of Pressure on Velocity of Burning. Nature, vol. 164, no. 4166, Sept. 3, 1949, pp. 403–404.
29. Gaydon, A. G., and Wolfhard, H. G.: Low-Pressure Flames and Flame Propagation. Fuel, vol. XXIX, no. 1, Jan. 1950, pp. 15–19.